American Mineralogist, Volume 87, pages 891–898, 2002

Fine structure of infrared OH-stretching bands in natural and heat-treated amphiboles of the tremolite-ferro-actinolite series

KIYOTAKA ISHIDA,[1,*] FRANK C. HAWTHORNE,[2] AND YUMI ANDO[1]

[1]Department of Evolution of Earth Environment, Graduate School of Social and Cultural Studies, Kyushu University, 4-2-1 Ropponmatsu, Chuo-ku, Fukuoka 810-8560, Japan

[2]Department of Geological Sciences, University of Manitoba, Winnipeg, Manitoba R3T 2N2, Canada

ABSTRACT

Fine structure in the principal OH-stretching bands of amphiboles of the tremolite-ferro-actinolite series have been examined. In samples with partly filled A sites, a broad (composite) band is observed at 3725~3680 cm^{-1} and is assigned to two types of configurations: (M1M1M3)-OH-^{A}(Na,K):^{T1}Si ^{T1}Al in which Al occurs at the T1 site, and (M1M1M3)-OH-^{A}(Na,K)-^{O3}(O^{2-},F^{-},Cl^{-}); the component of (M1M1M3)-OH-^{A}(Na,K):^{T1}Si ^{T1}Si configuration is small, because Na and K at the A site are locally associated with Al at an adjacent T1 site. In tremolite, manganoan tremolite, and Fe^{2+}-poor actinolite, a weak shoulder on the principal A band at ~3669 cm^{-1} is assigned to the configuration $^{M4}Ca^{M4}$(Mg,Fe^{2+},Mn^{2+},Na):(MgMgMg)-OH-^{A}□:^{T1}Si ^{T1}Si (□ = vacancy). Fine structure in the principal bands B (B' and B'') and C (C' and C'') are also observed: the higher-frequency band B'' is assigned to $^{M1}Fe^{2+}{}^{M1}Mg{}^{M3}$Mg-OH-^{A}□, and the lower-frequency band B' to $^{M1}Mg^{M1}Mg^{M3}Fe^{2+}$-OH-^{A}□; the higher-frequency band C' is assigned to $^{M1}Fe^{2+}{}^{M1}Fe^{2+}{}^{M3}$Mg-OH-^{A}□ and the lower-frequency band C'' to ^{M1}Mg $^{M1}Fe^{2+}{}^{M3}Fe^{2+}$-OH-^{A}□. Some broad OH-stretching bands attributed to (M1M1M3)-OH-^{A}□:^{T1}Si ^{T1}Al are observed at 3640~3580 cm^{-1}. In amphiboles of the tremolite-ferro-actinolite series that show a substantial B [(MgMgFe^{2+})-OH] band, a new OH-stretching band (at around 3641 cm^{-1}), E, appears near the principal C band (at around 3643 cm^{-1}) on heat treatment. The shape of band E is similar to that of the original band B, and its local configuration is O^{2-}-(MgMgFe^{3+})-OH^{-}. A weak and broad band A** appears at ~3690 cm^{-1} on heat treatment of some Na-bearing actinolites, and is ascribed to the (MgMgMg)-OH-^{A}Na-O^{2-} configuration.

INTRODUCTION

The hydroxyl group in the amphibole structure occupies the apex of a pseudotrigonal bipyramid, the base of which is formed by three cations at the two M1 and one M3 sites. The O-H vector lies along **a***, with the O-H bond projecting into the large cavity about the A site. For monoclinic amphiboles, a binary solid-solution (e.g., the tremolite-ferro-actinolite series) contains four chemically distinguishable NN (nearest-neighbor) configurations, with designated bands A to D: A = (MgMgMg), B = (MgMgFe^{2+}), C = (Mg$Fe^{2+}Fe^{2+}$), D = ($Fe^{2+}Fe^{2+}Fe^{2+}$) (Strens 1966; 1974). Detailed studies (Della Ventura et al. 1999; Hawthorne et al. 2000) have shown that the fine structure in the principal OH-stretching region is also affected by NNN (next-nearest-neighbor) cations at the M2, M4, T1, and A sites.

There are two tetrahedrally coordinated sites in the *C*2/*m* amphibole structure, T1 and T2. Normally, tetrahedrally coordinated Al is strongly ordered at the T1 site (Oberti et al. 1995a, 1995b). The effect of Al substitution at the T1 site on the infrared spectra of monoclinic amphiboles has been discussed by Della Ventura et al. (1999) and Hawthorne et al. (2000). There is hydrogen bonding between the H atom and the adjacent O7 anion. When O7 is bonded to Si and Al, the hydrogen bond to O7 must be stronger than when O7 is bonded to Si and Si. As the principal OH-stretching frequency is inversely related to the strength of the hydrogen bond, the presence of tetrahedrally coordinated Al gives rise to two bands: a higher-frequency band corresponding to ^{T1}Si^{T1}Si and a lower-frequency band corresponding to ^{T1}Si^{T1}Al.

Thus OH-stretching bands in the infrared region contain much information on chemical composition and short-range order, and several FTIR studies have shown that this is the case for amphiboles (e.g., Hawthorne et al. 1996a, 1996b, 2000; Della Ventura et al. 1999). However, the chemical compositions of amphibole-group minerals are frequently complicated, and FTIR spectroscopy has focused primarily on synthetic materials (e.g., Della Ventura et al. 1993, 1996a, 1996b, 1998; Gottschalk et al. 1998, 1999; Raudsepp et al. 1987; Robert et al. 1989, 1993; Najorka et al. 2000). In this paper, we report fine structure in the principal OH-stretching bands in natural amphiboles of the tremolite-ferro-actinolite series, and the appearance of new OH-stretching bands in their heat-treated counterparts.

MATERIAL EXAMINED AND EXPERIMENTAL METHODS

Eighteen samples were used for this study (Table 1), including chromium-bearing actinolite, chromium-bearing edenite, edenite, manganoan tremolite and manganoan actinolite. Experimental details for chemical analysis, ^{57}Fe Mössbauer spectroscopy and heat-treatment are those described by Ishida and Hawthorne (2001). Samples were prepared for infrared spectroscopy as 10 mm diameter ~200 mg KBr discs containing 4–9 mg of fine-grained amphibole. Infrared spectra were recorded in the range 4000–3000 cm^{-1} with a JASCO FTIR-

* E-mail: kiyota@rc.kyushu-u.ac.jp

620V spectrometer equipped with a DLATGS detector and a KBr beam splitter. Each sample was scanned 128 times in an evacuated sample-chamber at a nominal resolution of 1 cm^{-1}.

Results and discussion

Chemical composition

Chemical compositions and unit formulae are given in Table 2. Mössbauer spectra show that all Fe in manganoan tremolite (sample 42) is present as Fe^{3+}. Except for this sample, unit formula were calculated on the basis of 23 O atoms per formula unit (apfu) with total iron as FeO. The Fe^{3+}/Fe^{2+} ratios of samples F, 18, 19, and 21 were calculated from the Mössbauer data.

Infrared OH-stretching bands

Infrared spectra of untreated samples are shown in Figure 1. Each spectrum can be divided into three regions in descending or-

Table 1. Occurrance and mineral assemblages of amphiboles examined

No.: symbol	Mineral name: appearance	Occurrence: mineral assemblage*	Locality
A: MnAct	manganoan-actinolite: translucent, prismatic	regional & contact meta: Qtz+Rdn+Rds	Shimozuru mine, Miyazaki Pref. Japan
F: SkFac	ferroactinolite: dark-green, fiberous	skarn: Mag	Sakurago mine, Yamaguchi Pref. Japan
14: AkaishiEd	edenite: green, prismatic	reginal metamorphism: Di	Higashiakaishi, Ehime Pref. Japan
18: SanAct	actinolite: bluish-green, fiberous	skarn: Qtz	Sannotake, Fukuoka Pref. Japan
19: Act001	actinolite: deep green, prismatic	reginal metamorphism: Ep+Chl	Nishisonogi, Nagasaki Pref. Japan
21: Act005	actinolite: bluish green, prismatic	reginal metamorphism: Chl	Nishisonogi, Nagasaki Pref. Japan
22: AfgTr	tremolite: translucent, prismatic	?	Korano mujan, Afganistan
23: BrzAct	actinolite: bluish-green, fiberous	?	Gavernador Valadares, Minas Gerais, Brazil
25: FjFac	ferroactinolite: greenish, fiberous	skarn: Grt+Chl	Fujigatani mine, Yamaguchi Pref. Japan
36: Act2315	actinolite: bluish green, prismatic	reginal metamorphism: Chl	Nishisonogi, Nagasaki Pref. Japan
37: Tr007	tremolite: pale blue, prismatic	regional metamorphism: Dol	Nishisonogi, Nagasaki Pref. Japan
38: Act004	actinolite: bluish green, prismatic	regional metamorphism: Chl	Nishisonogi, Nagasaki Pref. Japan
39: CrAct	Cr-bearing actinolite: yellowish-green	regional metamorphism	Matsubase, Kumamoto Pref. Japan
40: CrEd	Cr-bearing edenite: pale green, prismatic	?	India
42: MnTr	manganoan-tremolite: pale-brown, prismatic	regional & contact metamorphism	Tirodi mine, Madhya Pradesh, India
58: InaTr	tremolite: translucent, fiberous	skarn	Inabe, Mie Pref. Japan
76: RaizAct4	actinolite: green, prismatic	regional metamorphism	Raizan, Itoshima, Fukuoka Pref. Japan
94: RaizAct6	actinolite: dark greenish-blue, prismatic	regional metamorphism: Ep	Raizan, Itoshima, Fukuoka Pref. Japan

* Mag = magnetite, Rdn = rhodonite, Rdc = rhodochrosite, Di = diopside, Qtz = quartz, Ep = epidote, Chl = chlorite, Grt = garnet, Phl = phlogopite, Dol = dolomite.

Table 2. Chemical compositions and structural formulae for amphiboles studied

No.	A	F	14	18	19	21	22	23	25	36	37	38
SiO_2	54.83	49.69	50.28	51.30	55.73	57.20	59.59	51.75	49.29	57.28	58.43	57.74
Al_2O_3	0.18	1.89	6.91	3.23	2.83	1.78	0.00	3.95	3.64	1.68	0.30	0.82
TiO_2	0.03	0.04	0.27	0.03	0.05	0.13	0.04	0.16	0.05	0.00	0.00	0.00
Cr_20_3	n.d.	n.d.	n.d.	n.d.	n.d.	n.d.	n.d.	n.d.	n.d.	n.d.	0.08	n.d.
MgO	15.07	4.15	16.54	11.46	17.77	20.25	23.62	15.32	6.88	20.24	23.43	20.44
FeO*	9.48	29.56	8.65	17.80	8.67	6.07	0.42	12.73	22.46	5.42	2.52	5.28
MnO	6.93	0.60	0.17	0.70	0.28	0.16	0.02	0.21	1.77	0.06	0.22	0.05
CaO	10.57	11.14	12.47	12.20	10.35	11.64	14.06	12.32	11.64	12.22	12.94	12.57
Na_2O	0.39	0.63	2.13	0.40	2.05	1.27	0.58	0.70	0.46	1.28	0.56	0.71
K_2O	0.04	0.15	0.62	0.15	0.12	0.07	0.03	0.20	0.17	0.06	0.02	0.00
Total	97.52	97.85	98.04	97.27	97.85	98.57	98.36	97.34	96.36	98.24	98.50	97.60
Si	7.981	7.785	7.181	7.637	7.832	7.885	8.041	7.514	7.625	7.905	7.946	8.000
Al	0.019	0.215	0.819	0.363	0.168	0.115	0.000	0.486	0.375	0.095	0.048	0.000
ΣT	8.000	8.000	8.000	8.000	8.000	8.000	8.041	8.000	8.000	8.000	7.994	8.000
Al	0.011	0.133	0.346	0.205	0.302	0.173	–	0.190	0.291	0.178	0.000	0.134
Ti	0.003	0.005	0.028	0.004	0.005	0.013	0.004	0.018	0.005	0.000	0.000	0.000
Cr^{3+}	–	–	–	–	–	–	–	–	–	–	0.009	–
Mg	3.256	0.967	3.520	2.542	3.721	4.161	4.750	3.316	1.578	4.164	4.749	4.221
Fe^{3+}	–	0.426	–	0.377	0.367	0.196	–	–	–	–	–	–
Fe^{2+}	1.166	3.447	1.034	1.840	0.652	0.503	0.048	1.546	2.915	0.626	0.287	0.611
Mn	0.564	0.022	0.021	0.032	–	–	0.002	–	0.211	0.007	–	0.005
ΣC	5.000	5.000	4.949	5.000	5.047	5.046	4.804	5.070	5.000	4.975	5.045	4.971
Mn	0.296	0.058	–	0.056	0.033	0.028	–	0.026	0.021	–	0.025	–
Ca	1.648	1.869	1.908	1.946	1.558	1.709	2.033	1.917	1.930	1.806	1.886	1.866
Na	0.056	0.073	0.092	0.000	0.409	0.263	0.000	0.057	0.049	0.194	0.089	0.134
ΣB	2.000	2.000	2.000	2.002	2.000	2.000	2.033	2.000	2.000	2.000	2.000	2.000
Na	0.049	0.116	0.498	0.116	0.151	0.076	0.150	0.141	0.088	0.150	0.058	0.058
K	0.009	0.030	0.111	0.029	0.021	0.013	0.005	0.038	0.034	0.010	0.003	0.000
ΣA	0.058	0.146	0.609	0.145	0.172	0.089	0.155	0.179	0.122	0.160	0.061	0.058
Lattice parameters												
a (Å)	9.8358(9)	9.9434(6)	9.8590(4)	9.8829(5)	9.8068(4)	9.8231(3)	9.8228(3)	9.8712(5)	9.9148(8)	9.8245(5)	9.8396(3)	9.8326(3)
b (Å)	18.149(2)	18.250(1)	18.0403(7)	18.1533(9)	18.0103(7)	18.0385(6)	18.0426(6)	18.1103(8)	18.217(1)	18.0436(8)	18.0567(5)	18.0510(6)
c (Å)	5.2953(5)	5.3102(4)	5.2889(2)	5.3030(3)	5.2927(2)	5.2834(2)	5.2736(2)	5.2969(3)	5.3083(5)	5.2825(3)	5.2768(2)	5.2802(2)
β (°)	104.386(6)	104.755(3)	104.872(2)	104.784(2)	104.617(2)	104.631(2)	104.676(2)	104.811(2)	104.741(4)	104.651(2)	104.695(2)	104.668(2)
V (Å^3)	915.6(2)	931.9(1)	909.18(6)	919.90(8)	904.55(6)	905.83(5)	904.14(5)	915.47(8)	927.2(1)	905.97(2)	906.86(5)	906.64(5)
asinβ (Å)	9.527	9.616	9.529	9.556	9.486	9.505	9.502	9.543	9.588	9.505	9.518	9.512

Note: n.d. = Not detected.
* Total iron as FeO.

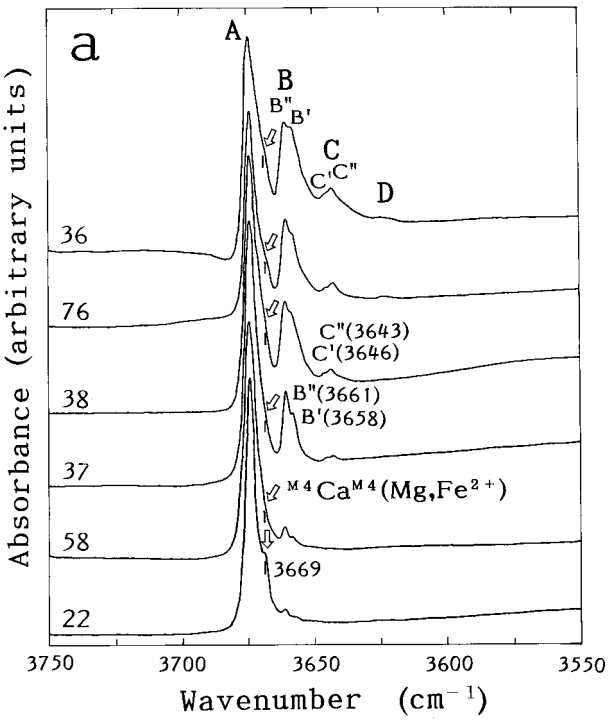

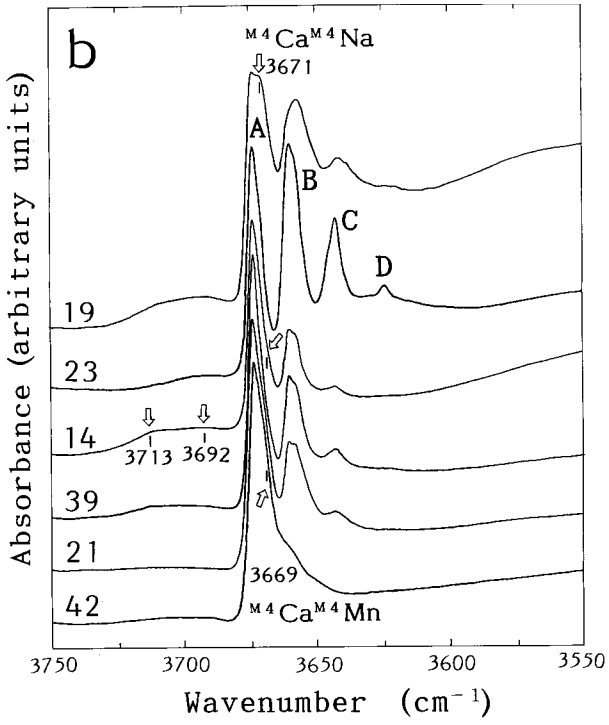

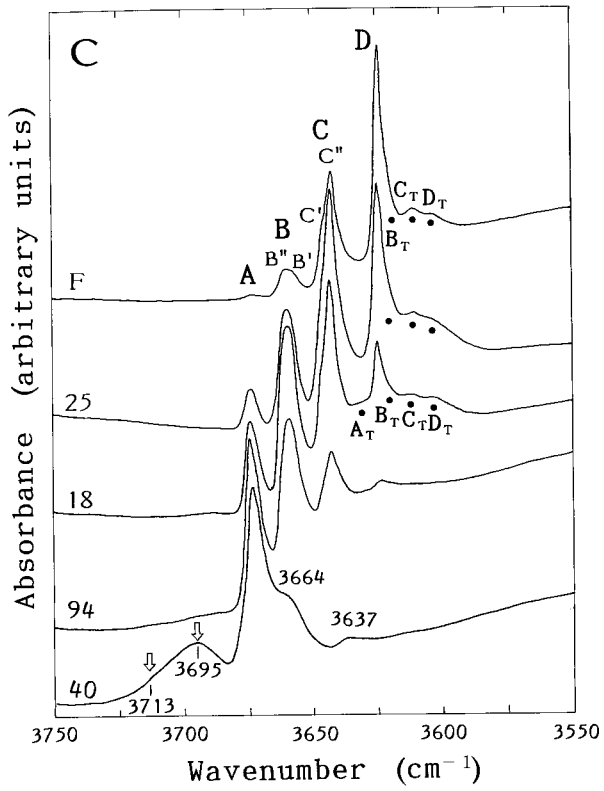

39	40	42	58	76	94
53.11	52.86	56.70	59.30	56.99	51.70
4.02	6.30	2.79	0.08	0.68	4.27
0.05	0.16	0.00	0.00	0.16	0.54
1.52	0.39	n.d.	n.d.	0.27	n.d.
19.79	22.78	21.12	24.16	19.64	14.41
4.98	0.14	3.27	0.32	6.05	12.37
0.06	0.00	2.73	0.07	0.14	0.31
12.50	12.57	11.00	14.20	13.10	12.40
0.46	2.77	2.05	0.00	0.66	0.98
0.11	0.27	0.18	0.08	0.03	0.28
96.60	98.24	99.84	98.21	97.72	97.26
7.502	7.238	7.728	8.006	7.951	7.514
0.498	0.762	0.272	–	0.049	0.486
8.000	8.000	8.000	8.006	8.000	8.000
0.172	0.255	0.176	0.013	0.063	0.245
0.005	0.017	0.000	0.000	0.016	0.059
0.169	0.042	–	–	0.030	–
4.166	4.650	4.292	4.863	4.085	3.122
–	–	0.373	–	–	–
0.587	0.016	–	0.036	0.706	1.504
–	0.000	0.159	0.008	0.016	0.038
5.099	4.980	5.000	4.920	4.916	4.968
0.007	0.000	0.156	–	–	–
1.892	1.845	1.606	2.054	1.957	1.931
0.101	0.155	0.238	–	0.043	0.069
2.000	2.000	2.000	2.054	2.000	2.000
0.024	0.580	0.304	0.000	0.136	0.206
0.020	0.046	0.031	0.014	0.004	0.052
0.044	0.626	0.335	0.014	0.140	0.258
9.8226(4)	9.8510(5)	9.8291(5)	9.8384(4)	9.8316(4)	9.8460(4)
18.0570(8)	18.0081(8)	18.0470(8)	18.0499(7)	18.0727(7)	18.0871(7)
5.2827(3)	5.2818(3)	5.2882(3)	5.2754(2)	5.2806(2)	5.2934(2)
104.726(2)	104.949(3)	104.612(3)	104.739(2)	104.671(2)	104.774(2)
906.20(7)	905.3(1)	907.71(8)	905.99(6)	907.68(6)	911.51(7)
9.500	9.518	9.511	9.515	9.511	9.520

FIGURE 1. Infrared OH-stretching spectra for amphiboles of the tremolite-ferro-actinolite series; (**a**) tremolite and Fe^{2+}-poor actinolite; (**b**) actinolite and ferro-actinolite having sub-stantial Na at the A site; (**c**) actinolite and ferro-actinolite.

der of frequency: (1) a composite band in samples with partly filled A sites; the configurations can be written as (M1M1M3)-OH-^{A}(Na,K):^{T1}Si ^{T1}(Si,Al) and (M1M1M3)-OH-^{A}(Na,K)-(O^{2-},F^{-},Cl^{-}) :^{T1}Si ^{T1}(Si,Al); (2) up to four main OH-stretching bands, A-D; these bands are assigned to configurations involving a vacant A site, and the configurations can be written as (M1M1M3)-OH-^{A}□:^{T1}Si^{T1}Si; (3) weak bands below ~3640 cm^{-1} (labeled A_T~D_T in Fig. 1c), though their intensity relations do not always coincide with those of the principal bands, A–D; their configurations are (M1M1M3)-OH-^{A}□:^{T1}Si^{T1}Al.

Fine structure due to partly filled A sites. The band ascribed to (MgMgMg)-OH-^{A}(Na,K):^{T1}Si^{T1}Si is observed at ~3735 cm^{-1} in synthetic and natural richterite, and that ascribed to (MgMgMg)-OH-^{A}Na:^{T1}Si^{T1}Al occurs at 3716 cm^{-1} in synthetic and natural pargasite (Hawthorne et al. 1997; Della Ventura et al. 1999; Melzer et al. 2000). Hawthorne et al. (1996a) showed that non-tremolite constituents in tremolite (i.e., Na, K, ^{T}Al, F) are not randomly distributed throughout the structure, but show extreme short-range order: Na and K at the A site are locally associated with Al at an adjacent T1 site. They assigned a weak 3730 cm^{-1} band to (MgMgMg)-(OH)-^{A}(Na,K):^{T1}Si^{T1}Si, a 3705 cm^{-1} band to (MgMgMg)-(OH)-^{A}(Na,K):^{T1}Si^{T1}Al, a 3674 cm^{-1} band to (MgMgMg)-OH-^{A}□:^{T1}Si^{T1}Si, and a broad <3649 cm^{-1} band to (MgMgMg)-OH-^{A}□: ^{T1}Si^{T1}Al.

Most of the tremolite-ferro-actinolite samples examined have negligible Na and K at the A site. The few samples that do have some ^{A}(Na,K) also have a broad band in the highest-frequency region (>3680 cm^{-1}) of their spectra (Fig. 1: 19, 14, 40). Inspection of the band envelopes in this region suggests the presence of two peaks at ~3710 and ~3695 cm^{-1}. The band at ~3710 cm^{-1} corresponds reasonably well with the 3705 cm^{-1} band assigned by Hawthorne et al. (1996a) to local association of ^{A}(Na,K) and ^{T1}Al around an MgMgMg-OH configuration. In accord with this assignment, the spectra with the most prominent signals in this region (14, 19, 40; Fig. 1) involve the amphiboles with the most ^{A}(Na,K) and ^{T}Al (Table 2). Thus the 3713 cm^{-1} band is assigned to (MgMgMg)-(OH)-^{A}Na:^{T1}Si^{T1}Al configuration in these spectra. Following Ishida and Hawthorne (2001), the 3695 cm^{-1} band is assigned to configurations of the type MgMgMg-OH-^{A}(Na,K)-^{O3}(O^{2-},F): ^{T1}Si^{T1}Al.

Fine structure in the A band. Jenkins (1987) showed that at least 5 mol% Mg substitutes for Ca at the M4 site in synthetic tremolite, and this has been confirmed by numerous subsequent studies (Ahn et al. 1991; Pawley et al. 1993; Maresch et al. 1994; Gottschalk et al. 1998, 1999; Hawthorne et al. 2000). In the infrared spectrum of synthetic tremolite, this Mg at the M4 site finds expression as a band (or bands) in the region of 3675 cm^{-1}, and Gottschalk et al. (1999) have shown that there is considerable fine-structure in this band due to different occupancy of the four M4 sites locally associated with each (OH) group. In the spectra of Figure 1, a shoulder on the principal A band is usually observed at ~3670 cm^{-1}, indicating significant substitution of other cations for Ca at M4, but no fine structure was observed.

Fine-structure in the B and C bands. The principal OH-stretching bands A and D are ascribed to the same types of cations, (MgMgMg) and ($Fe^{2+}Fe^{2+}Fe^{2+}$) in the tremolite-ferro-actinolite series, and hence there is no permutation broadening of these bands. On the other hand, the B and C bands correspond to the (Mg$Mg Fe^{2+}$)-OH-^{A}□:^{T1}Si^{T1}Si and (Mg$Fe^{2+}Fe^{2+}$)-OH-^{A}□:^{T1}Si^{T1}Si configurations, and hence should show permutation broadening (Strens 1966, 1974). Using a notation similar to that of Strens (1974), the band B is composed of B' and B" bands; the associated configurations are ^{M1}Mg ^{M1}Mg $^{M3}Fe^{2+}$ and $^{M1}Fe^{2+}$ ^{M1}Mg ^{M3}Mg, respectively, and the intensity of the B" band must be twice that of the B' band (Fig. 2). These B' and B" bands are visible in Figure 1a, and from their intensity relations, we can recognize that the frequency of B" (3661 cm^{-1}) is higher than that of B' (3658 cm^{-1}). Similarly, the C band is composed of C' and C" bands; the associated configurations are $^{M1}Fe^{2+}$ $^{M1}Fe^{2+}$ ^{M3}Mg and ^{M1}Mg $^{M1}Fe^{2+}$ $^{M3}Fe^{2+}$, respectively, and the intensity of band C" must be twice that of band C' (Fig. 2). Although the intensities of the C' and C" bands are weak in Figure 1a, it is clear that the frequency of C' (3646 cm^{-1}) is higher than that of C" (3643 cm^{-1}). With increasing Fe^{2+}, Fe^{3+}, Al, and Na in the amphibole, this fine-structure becomes obscured; however, unsymmetrical behavior is still apparent in the B and C bands (Fig. 1c).

Mössbauer spectra and infrared OH-stretching bands of heat-treated samples

Mössbauer spectra of selected untreated (U.T.) and heat-treated samples are shown in Figures 3, 4, and 5. The changes in the Mössbauer spectra in these amphiboles are similar to those reported by Whitfield and Freeman (1967), Ernst and Wai (1970), Ishida (1998, 1999) and Ishida and Hawthorne (2001). Infrared spectra for untreated and heat-treated tremolite-ferro-actinolites samples are shown in Figure 6. The changes in the OH-stretching bands on heating in these amphiboles are simi-

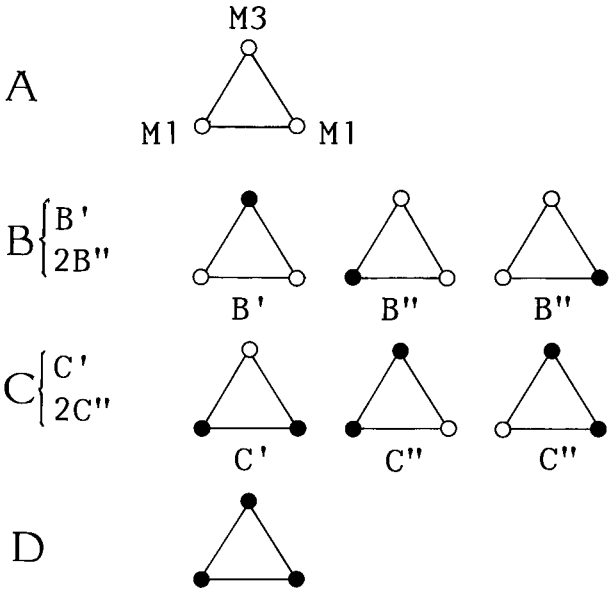

FIGURE 2. Possible short-range assignments of Mg (open circles) and R^{2+} (R = transition elements such as Fe and Mn; solid circles) over the M1 and M3 sites in amphibole.

lar to those reported by Ernst and Wai (1970), Ishida (1999), and Ishida and Hawthorne (2001).

Mössbauer spectra of heat-treated samples

In the spectra of untreated samples (Figs. 3a, 4a, and 5a), the outer *AA*' doublet is due to Fe^{2+} at the M1and M3 sites, and *BB*' is due to Fe^{2+} at the M2 site; the *CC*' doublets are due to Fe^{3+} at the M2 site (Hawthorne 1983, 1988 and references therein). Although the low-velocity component (*C*) of the *CC*' doublet overlaps with the low-velocity components of the *AA*' and *BB*' doublets, the presence or absence of Fe^{3+} can be recognized by the presence or absence of the high-velocity (*C*') component of the *CC*' doublet at 0.7 mm/s. With increasing temperature of treatment, the intensities of the *AA*' and *BB*' doublets decrease and the *DD*' and *EE*' doublets appear. The inner doublet *DD*', with smaller quadrupole splitting (QS) and larger isomer shift (IS), is attributed to Fe^{3+} at the M1 and M3 sites, and the outer doublet *EE*', with larger QS and smaller IS, is attributed to Fe^{3+} at M2. The *CC*' doublet overlaps with the *DD*' doublet, and these doublets cannot be resolved. In some Fe^{2+}-containing samples, oxidation of Fe^{2+} occurs more rapidly at the M1 and M3 sites than at the M2 site (Figs. 3 and 5), as Fe^{2+} at the M1 and M3 sites can participate in a NN (nearest-neighbor) coupled oxidation-dehydrogenation reaction with OH molecules at the locally associated O3 sites. For samples with small amounts of Fe^{2+}, coupled dehydrogenation-oxidation consumes all Fe^{2+} (Fig. 4). However, for samples with large amounts of Fe^{2+}, some Fe^{2+} remains at M2 (*BB*' doublet) until the sample breaks down at higher temperature (Fig. 5d).

Infrared spectra of heat-treated samples

Appearance of band E. Oxidation-dehydrogenation proceeds via the reaction (Ernst and Wai 1970):

$$^{M1,M3}Fe^{2+} + {}^{O3}(OH)^{-} = {}^{M1,M3}Fe^{3+} + {}^{O3}O^{2-} + H\uparrow \quad (1)$$

Thus the A = (MgMgMg)-OH band persists up to high temperature, and the intensities of the B-D bands decrease and finally disappear via the reactions:

$$\text{B-band: } (MgMgFe^{2+}) + 2\ {}^{O3}(OH)^{-} = (MgMgFe^{3+}) + {}^{O3}(OH)^{-} + {}^{O3}O^{2-} + H\uparrow \quad (2)$$

$$\text{C-band: } (MgFe^{2+}Fe^{2+}) + 2\ {}^{O3}(OH)^{-} = (MgFe^{3+}Fe^{3+}) + 2\ {}^{O3}O^{2-} + 2H\uparrow \quad (3)$$

$$\text{D-band: } (Fe^{2+}Fe^{2+}Fe^{2+}) + 2\ {}^{O3}(OH)^{-} = (Fe^{2+}Fe^{3+}Fe^{3+}) + 2\ {}^{O3}O^{2-} + 2H\uparrow \quad (4)$$

With heating at higher temperature, remaining $^{O3}(OH)$ in the dehydrogenated B-type configuration 2, and the OH from an A-band configuration react either with Fe^{2+} of the completely

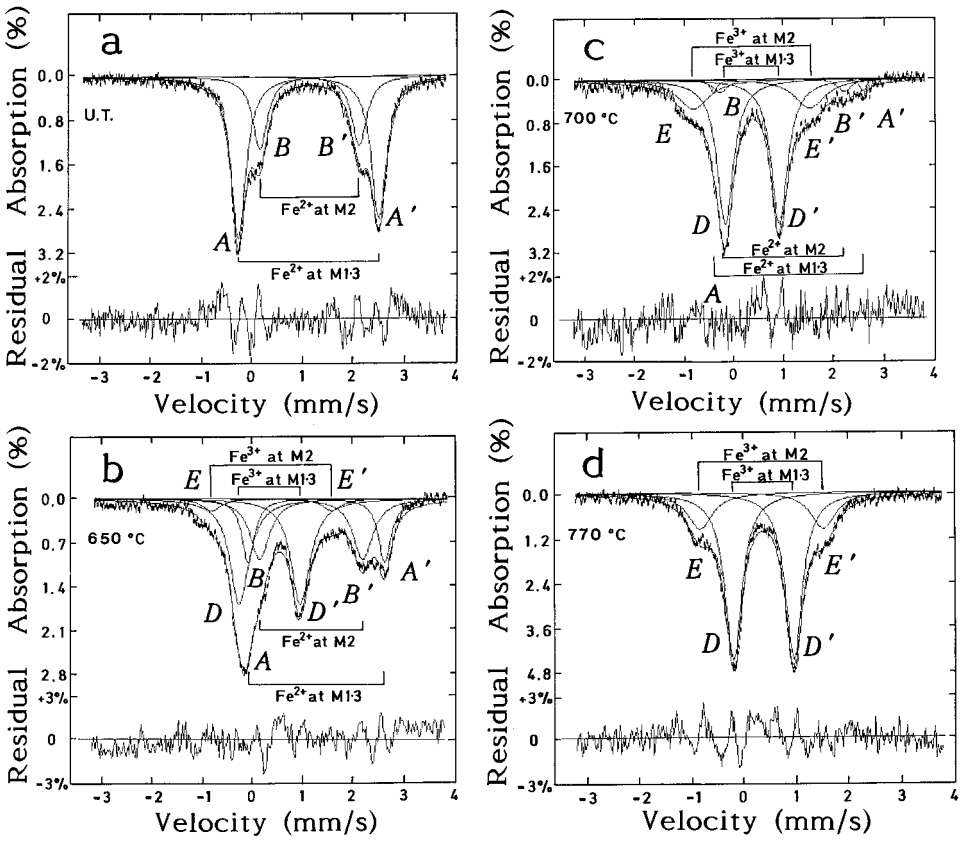

FIGURE 3. Mössbauer spectra of manganoanactinolite (sample A) heat-treated in air.

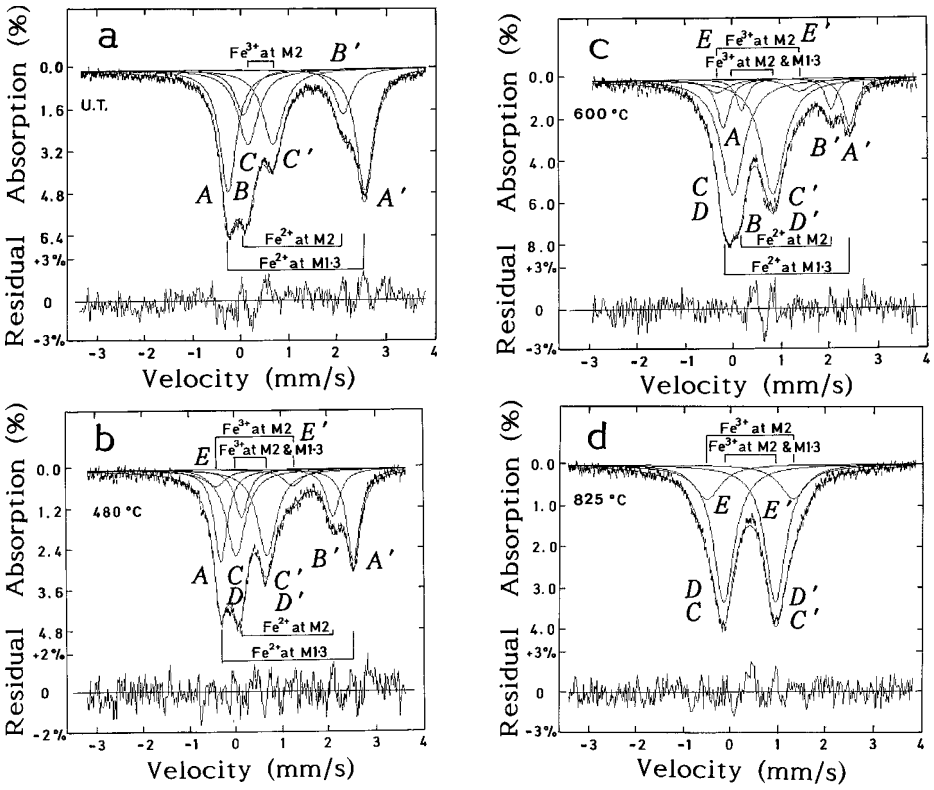

FIGURE 4. Mössbauer spectra of actinolite (sample no.19) heat-treated in air.

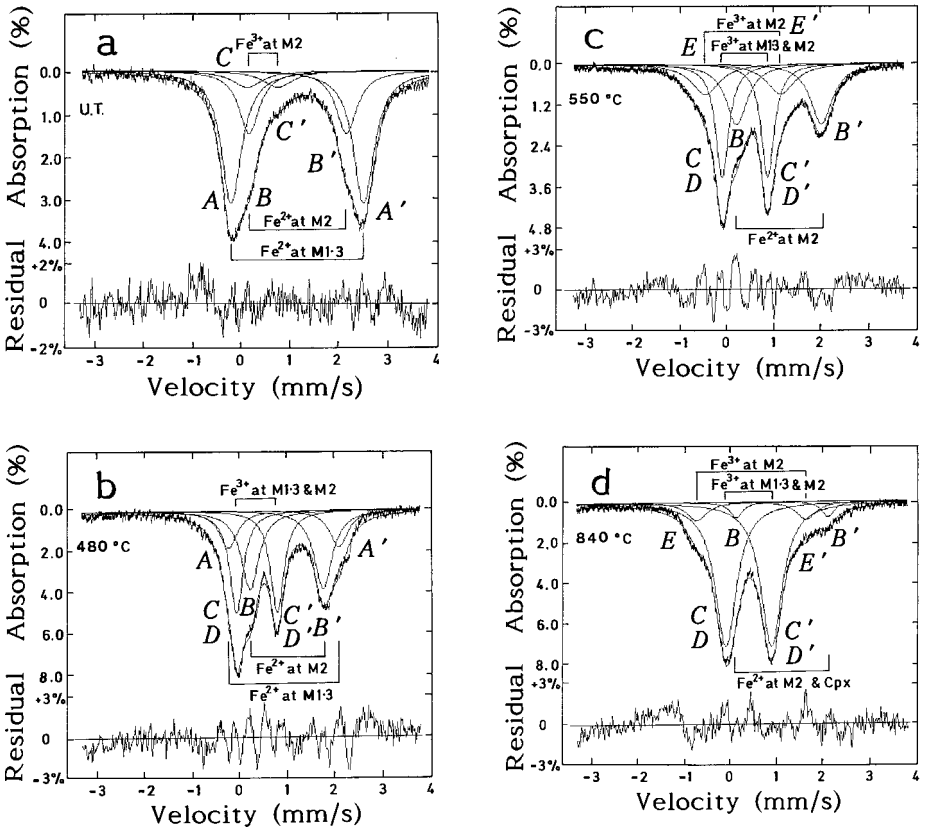

FIGURE 5. Mössbauer spectra of ferro-actinolite (sample F) heat-treated in air.

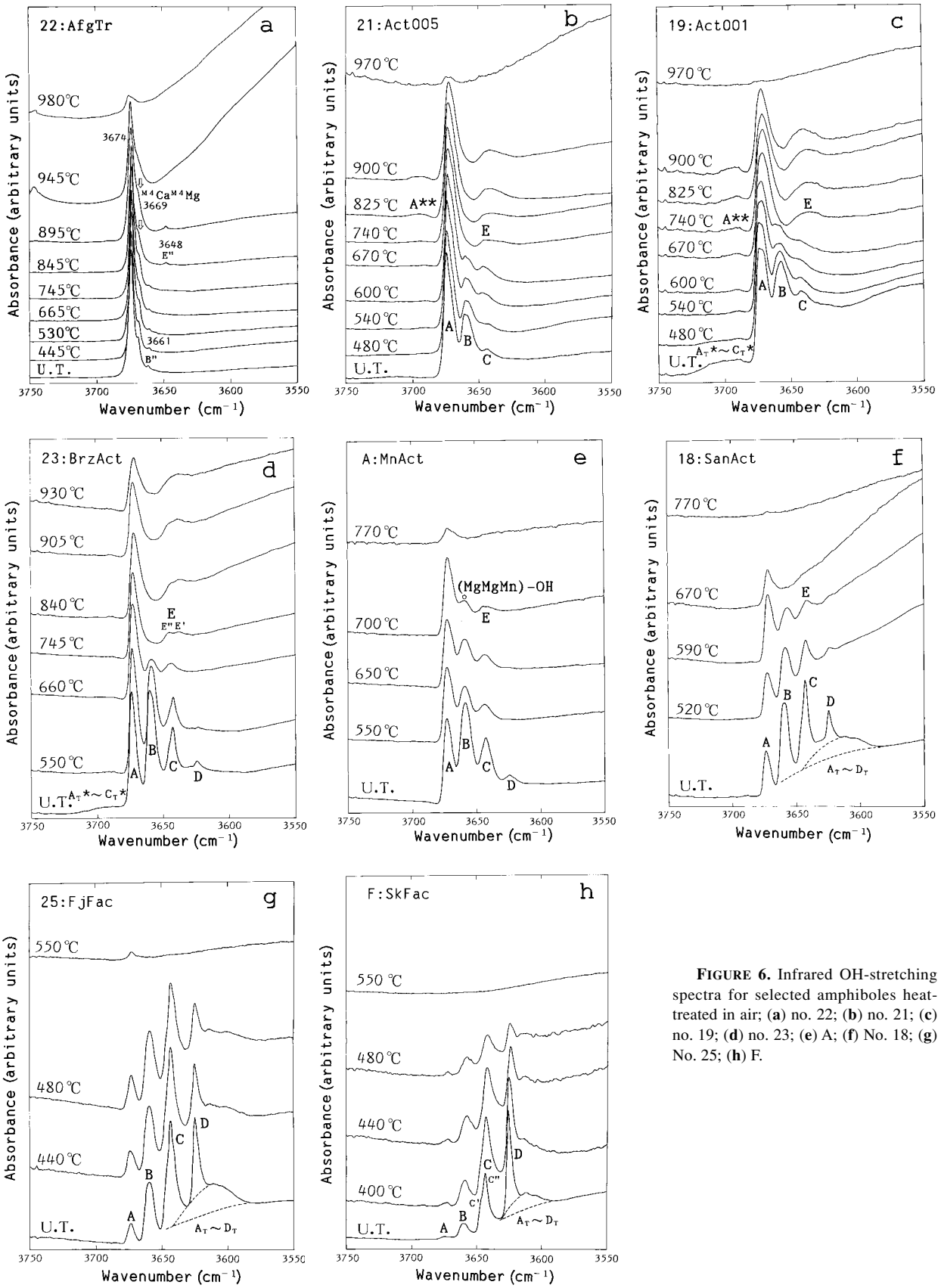

FIGURE 6. Infrared OH-stretching spectra for selected amphiboles heat-treated in air; (**a**) no. 22; (**b**) no. 21; (**c**) no. 19; (**d**) no. 23; (**e**) A; (**f**) No. 18; (**g**) No. 25; (**h**) F.

dehydrogenated D-type configuration 4, or with Fe^{2+} at the M2 or M4 sites. For samples in which O3 is completely occupied by OH and which contain more than 2.0 apfu Fe^{2+}, up to 2.0 apfu Fe^{2+} are consumed during oxidation-dehydrogenation, and almost all of the OH-stretching bands disappear below ~700 °C (Figs. 6g and 6h). During oxidation-dehydrogenation affecting the B band, (Eq. 2), a broad OH-stretching band, E, appears near band C, shifted downward due to the electronegativity difference between Fe^{2+} and Fe^{3+}. Although the frequency of this band is close to that of band C, it is ascribed to $(MgMgFe^{3+})$-OH and its local configuration is O^{2-}-$(MgMgFe^{3+})$-OH, as shown in (Eq. 2). Moreover, the band broadens and it is clear that this band has two components, E' and E'': E' = $^{M1}Mg^{M1}Mg^{M3}Fe^{3+}$ and E'' = $^{M1}Fe^{3+}\,{}^{M1}Mg^{M3}Mg$, and their frequency relation is the same as that of band B: E'' has a higher frequency than E' by ~8 cm^{-1}. In samples with less than 2.0 apfu Fe^{2+}, A and E bands persist above 900 °C (Figs. 6a, 6b, 6c, and 6d).

Appearance of band A.** With increasing temperature of heat treatment, a weak broad band appears at ~3690 cm^{-1} in some actinolite samples (A** in Figs. 6b and 6c). These samples contain 0.194 and 0.409 Na apfu, respectively, at M4, and also 0.150 and 0.246 Na apfu, respectively, at the A site. Following the discussion given above for unheated natural samples, the A** band is attributed to the configuration (M1M1M3)-OH-^{A}(Na,K):$^{T1}Si^{T1}Al$, associated with O^{2-} at the O3 site across the A cavity [i.e., (MgMgMg)-OH-^{A}Na-$^{O3}O^{2-}$]. The intensity of this band increases during heat-treatment because both $^{O3}O^{2-}$ and ^{A}Na are increasing; ^{A}Na increases because of migration from the M4 site.

ACKNOWLEDGMENTS

The authors thank M. Akasaka and I. Shinno for their kind permission to use their program for fitting Mössbauer spectra. We are also grateful to Y. Aoki, Y. Kuwahara, D. M. Jenkins, G. Della Ventura, and M. Koch-Müller for their reviews of this manuscript. Infrared spectra were recorded at the Center of Advanced Instrumental Analysis, Kyushu University. Part of this work was done during the stay of KI at the Department of Geological Sciences, University of Manitoba, Winnipeg, supported by a grant from the International Council for Canadian Studies.

REFERENCES CITED

Ahn, J.H., Cho, M., Jenkins, D.M., and Buseck, P.R. (1991) Structural defects in synthetic tremolitic amphiboles. American Mineralogist, 76, 1811–1823.

Della Ventura, G., Robert, J.-L., Raudsepp, M., and Hawthorne, F.C. (1993) Site occupancies in monoclinic amphiboles: Rietveld structure refinement of synthetic nickel magnesium cobalt potassium richterite. American Mineralogist, 78, 633–640.

Della Ventura, G., Robert, J.-L., Hawthorne, F.C., and Prost, R. (1996a) Short-range disorder of Si and Ti in the tetrahedral double-chain unit of synthetic Ti-bearing potassium-richterite. American Mineralogist, 81, 56–60.

Della Ventura, G., Robert, J.-L., and Hawthorne, F.C. (1996b) Infrared spectroscopy of synthetic (Ni,Mg,Co)-potassium-richterite. In M.D. Dyar, C. McCammon, and M.W. Schaefer, Eds., Mineral Spectroscopy: A Tribute to Roger G. Burns, p. 55–63. The Geochemical Society Special Publication No. 5. St. Louis, MO.

Della Ventura, G., Robert, J.-L., Hawthorne, F.C., Raudsepp, M., and Welch, M.D. (1998) Contrasting patterns of $^{[6]}$Al order in synthetic pargasite and Co-substitued pargasite. Canadian Mineralogist, 36, 1237–1244.

Della Ventura, G., Hawthorne, F.C., Robert, J.-L., Delbove, F., Welch, M.F., and Raudsepp, M. (1999) Short-range order of cations in synthetic amphiboles along the richterite-pargasite join. European Journal of Mineralogy, 11, 79–94.

Ernst, W.G. and Wai, C.M. (1970) Mössbauer, infrared, X-ray and optical study of cation ordering and dehydrogenation in natural and heat-treated sodic amphiboles. American Mineralogist, 55, 1226–1256.

Gottschalk, M., Andrut, M., and Melzer, S. (1999) The determination of the cummingtonite content of synthetic tremolite. European Journal of Minerlogy, 11, 967–982.

Gottschalk, M., Najorka, J., and Andrut, M. (1998) Structural and compositional characterization of synthetic (Ca, Sr)-tremolite and (Ca, Sr)-diopsides. Physics and Chemistry of Minerals, 25, 415–428.

Hawthorne, F.C. (1983) The crystal chemistry of the amphiboles. Canadian Mineralogist, 21, 173–480.

———(1988) Mössbauer spectroscopy. Reviews in Mineralogy, 18, 255–340.

Hawthorne, F.C., Della Ventura, G., and Robert, J.-L. (1996a) Short-range order of (Na,K) and Al in tremolite: An infrared study. American Mineralogist, 81, 782–784.

———(1996b) Short-range order and long-range order in amphiboles: a model for the interpretation of infrared spectra in the principal OH-stretching region. In M.D. Dyar, C. McCammon and M.W. Schaefer, Eds., Mineral Spectroscopy: A Tribute to Roger G. Burns, 49–54. The Geochemical Society, Special Publication No. 5. St. Louis, MO.

Hawthorne, F.C., Della Ventura, G.D., Robert, J.-L., Welch, M.D., Raudsepp, M., and Jenkins, D.M. (1997) A Rietveld and infrared study of synthetic amphiboles along the potassium-richterite-tremolite join. American Mineralogist, 82, 708–716.

Hawthorne, F.C., Welch, M.D., Della Ventura, G.D., Liu, S., Robert, J.-L., and Jenkins, D.M.(2000) Short-range order in synthetic aluminous tremolites: An infrared and triple-quantum MAS NMR study. American Mineralogist, 85, 1716–1724.

Ishida, K. (1998) Cation disordering in heat-treated anthophyllites through oxidation and dehydrogenation. Physics and Chemistry of Minerals, 25, 160–167.

———(1999) Appearance of infrared $(MgMgFe^{3+})$-OH stretching band in heat-treated holmquistites, sodic-calcic and sodic amphiboles. Mineralogical Journal, 21, 157–166.

Ishida, K. and Hawthorne, F.C. (2001) Assignment of infrared OH-stretching bands in manganoan magnesio-arfvedsonite and richterite through heat-treatment. American Mineralogist, 86, 965–972.

Jenkins, D.M. (1987) Synthesis and characterization of tremolite in the system H_2O-CaO-MgO-SiO_2. American Mineralogist, 72, 707–715.

Maresch, W.V., Czank, M., and Schreyer, W. (1994) Growth mechanisms, structural defect and composition of synthetic tremolite: what are the effects on microscopic properties? Contributions to Mineralogy and Petrology, 118, 297–313.

Melzer, S., Gottschalk, M., Andrut, M., and Heinrich, W. (2000) Crystal chemistry of K-richterite-richterite-tremolite solid solutions: a SEM, EMP, XRD, HRTEM and IR study. European Journal of Mineralogy, 12, 273–291.

Najorka, J., Gottschalk, M., and Heinrich, W. (2000) Structural and thermo-dynamic properties of the synthetic tremolite-magnesiohornblende solid solutions. Eighth International Symposium on Experimental Mineralogy, Petrology and Geochemistry, Journal of Conference Abstracts, 5–1, 77.

Oberti, R., Hawthorne, F.C., Ungaretti, L., and Cannillo, E. (1995a) ^{VI}Al disorder in amphiboles from mantle peridotites. Canadian Mineralogist, 33, 867–878.

Oberti, R., Ungaretti, L., and Cannillo, E., Hawthorne, F.C., and Memmi, I. (1995b) Temperature-dependent Al order-disorder in the tetrahedral double chain of C2/m amphiboles. European Journal of Mineralogy, 7, 1049–1063.

Pawley, A.R., Graham, C.M., and Navrotsky, A. (1993) Tremolite-richterite amphiboles: Synthesis, compositional and structural characterization and thermochemistry. American Mineralogist, 78, 23–35.

Raudsepp, M., Turnock, A.C., Hawthorne, F.C., Sherriff, B.L., and Hartman, J.S. (1987) Characterization of synthetic pargasitic amphiboles ($NaCa_2Mg_4M^{3+}Si_6Al_2O_{22}(OH,F)_2$; M^{3+} = Al, Cr^{3+}, Ga, Fe^{3+}, Sc, In) by infrared spectroscopy, Rietveld structure refinement and ^{27}Al and ^{29}Si MAS NMR spectroscopy. American Mineralogist, 72, 580–593.

Robert, J.-L., Della Ventura, G.C., and Thauvin, J.-L. (1989) The infrared OH-stretching region of synthetic richiterites in the system Na_2O-K_2O-CaO-MgO-SiO_2-H_2O-HF. European Journal of Mineralogy, 1, 203–211.

Robert, J.-L., Della Ventura, G., Raudsepp, M., and Hawthorne, F.C. (1993) Rietveld structure refinement of synthetic strontium-rich potassium-richterites. European Journal of Mineralogy, 5, 199–206.

Strens, R.G.J. (1966) Infrared study of clustering and ordering in some (Fe, Mg) amphibole solid solutions. Chemical Communications, 519.

———(1974) The common chain, ribbon, and ring silicates. In V.C. Farmer, Ed., The infrared spectra of minerals. Mineralogical Society, London, U.K.

Whitfield, H.J. and Freeman, A.G. (1967) Mössbauer study of amphiboles. Journal of Inorganic Nuclear Chemistry, 29, 903–914.

MANUSCRIPT RECEIVED APRIL 16, 2001
MANUSCRIPT ACCEPTED FEBRUARY 8, 2002
MANUSCRIPT HANDLED BY ROBERTA OBERTI

View publication stats